Aerodynamics of Flutter

Department of Mechanics

May 18, 2011

Author:
Emelie Barman

Supervisor:
Hanno Essén

Abstract

The unsteady flow around an aerofoil placed in a uniform flow stream with an angle of attack is investigated, under the assumption of inviscid, incompressible, two-dimensional flow. In particular, a function of the velocity jump over the wake is achieved, where this function depends on the horizontal displacement and time. The aerofoil geometry is represented by two arbitrary functions, one for the upper and one for the lower side of the aerofoil. These functions are dependent on time, hence the aerofoil can perform oscillating movement, which is the case when subjected to flutter.

The governing equations for the flow are the Euler equations. By assuming thin aerofoil, small angle of attack and that the perturbation of the wake is small, the problem is linearised. It is shown that the linearised Euler equations can be rewritten as the Cauchy-Riemann equations, and an analytic function exists where its real part is the horizontal velocity component and its imaginary part is the vertical velocity component with opposite sign.

The flow field is then investigated in the complex plane by making an appropriate branch cut removing all discontinuities, and with restrictions on the analytic function such that the kinematic and boundary conditions are satisfied. By using Cauchy's integral formula an expression for the anti-symmetric part of the analytic function is achieved. A general expression for the velocity jump over the wake is obtained, which is applied to the specific case of harmonic oscillations for a symmetric aerofoil. In the end three types of flutter is investigated; twisting oscillations around the centre of stiffness, vertical oscillation, and aileron flutter.

Sammanfattning

Det tidsberoende strömningsflödet runt en vingprofil placerad i en konstant friströmshastighet är undersökt under antagandet av friktionsfri, inkompressibel två-dimensionell strömning. En funktion för hastighetshoppet över vaken tas fram, där funktionen beror av den horisontella positionen samt tiden. Vingprofilens geometri beskrivs av två godtyckliga funktioner, en för översidan och en för undersidan. Funktionerna är tidsberoende vilket möjliggör oscillerande rörelser, vilket är fallet när vingprofilen är utsatt för fladder.

De styrande ekvationerna för strömningen runt vingprofilen är Eulerekvationerna. Genom antagandet av tunn vingprofil, liten anfallsvinkel samt att störningen av vaken är liten linjäriseras problemet. Det visas att de linjäriserade Eulerekvationerna kan skrivas om som Cauchy-Riemannekvationerna, varav det existerar en analytisk funktion vars realdel utgör den horisontella hastighetskomponenten och imaginärdel utgör den vertikala hastighetskomponenten med ombytt tecken.

Strömningen runt vingprofilen är sedan undersökt i det komplexa talplanet genom ett lämpligt val av snitt för att ta bort alla diskontinuiteter i planet, samt med villkor på den analytiska funktionen så att de kinematiska villkoren samt randvillkoren är uppfyllda. Genom att använda Cauchys integralformel tas ett uttryck för den anti-symmetriska delen av den analytiska funktionen fram. Ett generellt uttryck för hastighetshoppet över vaken tas fram, vilket sedan tillämpas på det specifika fallet för harmonisk svängning av en symmetrisk vingprofil. Slutligen analyseras tre fall av fladder; vridande svängning runt styvhetscentrum, vertikal svängning samt skevrodsfladder.

Acknowledgements

I would like to thank my supervisor Prof. A. I. Ruban, at Imperial Collage London where the thesis was done, for the consistent support, help and guidance throughout the project. Furthermore, I am very thankful for the support given by my friends Jeroen Van den Eynde and Tobias Plaumann during the project, and the support given by Pär Lorentz and Fredrik Hansson during my entire degree.

Contents

Chapter 1

Introduction

The aeroelastic phenomenon flutter is a structural dynamical instability which can happen to any elastic structure, making the structure vibrate violently with increasing amplitude. It is due to the interaction of the elastic and inertial forces of the structure with the unsteady aerodynamic forces generated by the oscillating motion of the structure, hence is a self-excited oscillation. The energy of the airstream is transferred to the structure and transformed into mechanical vibrations, leading to an increase of the amplitude of the oscillations. If the airstream velocity is high enough the structural damping is not strong enough to damp out the oscillations, which can lead to failure. Flutter is therefore very dangerous and the area very important. In this report only the aerodynamic response is investigated and not the structural.

In this report the two-dimensional unsteady flow field obtained by placing an unsteady aerofoil with arbitrary shape in a uniform flow with angle of attack is analysed. Since flutter is of interest the aerofoil shape is dependent of both time and horizontal displacement, to make oscillating movements possible. Further the flow is assumed to be inviscid and incompressible, and the governing equations for the flow field reduce to the unsteady Euler equations. When the aerofoil performs oscillations in the flow field circulation will be generated and, hence lift. According to Helmholtz's theorem the total circulation around the aerofoil must be constant, and therefore for each time-depending change of circulation due to the oscillating movements vortices are shed from the trailing edge to compensate[1]. This generates a wake after the aerofoil. In the inviscid case this wake will only be a discontinuity line in the form of a velocity jump. The main purpose of the project is to find a function for this velocity jump.

Chapter 2

Literature review

In 1922, the general stationary thin-aerofoil problem was determined by Munk [2], where he derived the normal force and moment on a thin aerofoil of arbitrary shape. Further on, in the late twenties and mid thirties Glauert [4] and Theodorsen [3] made valuable contributions in the unsteady thin-aerofoil theory, where flat thin aerofoils with trailing edge flaps undergoing heaving and pitching motion where analysed and the lift and moment were derived. These are still of great importance as analytical and numerical investigations of unsteady aerodynamic forces on oscillating airfoils are often based on the two-dimensional potential-flow model used in Theodorsen's work [20]. For the case when neither the aerofoil or the trailing edge flap is flat, more computationally costly methods have been used, such as the discrete vortex method by of Katz [5, 6] and full Navier-Stokes methods as in van der Wall [7].

The unsteady flow field that occurs when a stationary aerofoil in a potential flow is subjected to a convected sinusoidal gust is investigated in the work of M. E. Goldstein and H. Atassi [8].

The investigation of the unsteady flow field as a response to a thin oscillating aerofoil in an oncoming flow is not restricted to an analysis of flutter only. In fact, there are several areas within this analysis of great importance. One example is swimming of fish, or fish propulsion. This is of big interest within the marine industry, to be able to find new forms of marine propulsion and maneuvering.

M. S. Triantafyllou, G. S. Triantafyllou and D. K. P. Yue are in their paper [9] discussing the area saying that experiments and theoretical work for producing propulsive forces in oscillating bodies and fins in water is of great importance. The propulsive efficiency of harmonically waving two-dimensional thin plates have been investigated by Wu [22, 23], where pressure and integrals over the surface shape as well as leading edge force singularity in time and space is analysed. Further, the unsteady leading edge suction force has been studied by Garrick [7] to be able to investigate the propulsive efficiency of oscillatory heaving, pitching and TE-flapping motions of a flat airfoil with a flat flap.

The deformation of aerofoils can as well be applied to the field of wind energy, where a new technique using piezoelectric materials makes it possible to have active flow control by deformation of aerofoil shapes.

Chapter 3

Defining problem

3.1 Formulation

A thin aerofoil is placed in an two-dimensional uniform, inviscid, incompressible flow with angle of attack α. The coordinate system is placed with the origin at the leading edge of the aerofoil, with $\hat{x}$ denoting the displacement in the horizontal direction and $\hat{y}$ the displacement in the vertical direction. The projection of the velocity vector upon these axes are denoted $\hat{u}$ and $\hat{v}$ respectively. The incidence α is defines as the angle between the free stream velocity vector and the $\hat{x}$-axis. The notation $\hat{}$ indicates dimensional variables.

In the far distance the unperturbed flow field is defined by the pressure p_∞, density ρ and free stream velocity U_∞. The chord length is c and as a measure of the aerofoil thickness a non-dimensional parameter ε is used, defined as the quotient of the maximum thickness of the aerofoil and the length of the chord. This parameter is small since the aerofoil is assumed thin.

Due to the unsteady flow field a wake is generated after the aerofoil. In the inviscid case this is only a velocity jump in the form of a discontinuity line. The wake starts at the trailing edge and will with time grow. The end of the wake travels with the free stream velocity U_∞, hence will be at the position $c + U_\infty \hat{t}$ in the $\hat{x}$-direction at time $\hat{t}$. Figure 3.1 shows the layout of the flow.

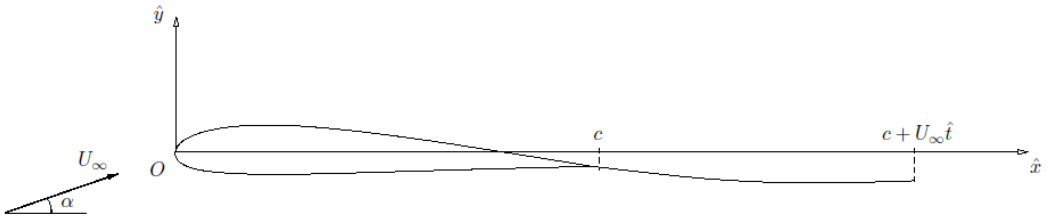

Figure 3.1: Incompressible, inviscid flow past a thin aerofoil with wake.

3.1.1 The Euler equations and boundary conditions

In a flow past an aerofoil the governing equations for the motion of the flow field will be the Navier-Stokes equations. Incompressible inviscid unsteady flow in two-dimensions leads to that the Navier-Stokes equations reduce to the unsteady two-dimensional Euler equations

$$\frac{\partial \hat{u}}{\partial \hat{t}} + \hat{u}\frac{\partial \hat{u}}{\partial \hat{x}} + \hat{v}\frac{\partial \hat{u}}{\partial \hat{y}} = -\frac{1}{\rho}\frac{\partial \hat{p}}{\partial \hat{x}} \tag{3.1a}$$

$$\frac{\partial \hat{v}}{\partial \hat{t}} + \hat{u}\frac{\partial \hat{v}}{\partial \hat{x}} + \hat{v}\frac{\partial \hat{v}}{\partial \hat{y}} = -\frac{1}{\rho}\frac{\partial \hat{p}}{\partial \hat{y}} \tag{3.1b}$$

$$\frac{\partial \hat{u}}{\partial \hat{x}} + \frac{\partial \hat{v}}{\partial \hat{y}} = 0 \tag{3.1c}$$

Far away from the aerofoil the flow field will not be affected by the aerofoil and the flow will coincide with the free stream velocity, hence the boundary conditions in the far distance will be

$$\left.\begin{aligned} \hat{u} &= U_\infty \cos\alpha \\ \hat{v} &= U_\infty \sin\alpha \\ \hat{p} &= p_\infty \end{aligned}\right\} \quad \text{at } \hat{x}^2 + \hat{y}^2 = \infty \tag{3.2}$$

These equations are now written in a non-dimensional form using non-dimensional variables according to

$$\begin{cases} \hat{x} = cx \\ \hat{y} = cy \\ \hat{u} = U_\infty u \\ \hat{v} = U_\infty v \\ \hat{p} = p_\infty + \rho U_\infty^2 p \\ \hat{t} = \frac{c}{U_\infty} t \end{cases} \tag{3.3}$$

Substituting (3.3) into (3.1) and (3.2) gives the non-dimensional Euler equations

$$\frac{\partial u}{\partial t} + u\frac{\partial u}{\partial x} + v\frac{\partial u}{\partial y} = -\frac{\partial p}{\partial x} \tag{3.4a}$$

$$\frac{\partial v}{\partial t} + u\frac{\partial v}{\partial x} + v\frac{\partial v}{\partial y} = -\frac{\partial p}{\partial y} \tag{3.4b}$$

$$\frac{\partial u}{\partial x} + \frac{\partial v}{\partial y} = 0 \tag{3.4c}$$

with boundary conditions

$$\left.\begin{aligned} u &= \cos\alpha \\ v &= \sin\alpha \\ p &= 0 \end{aligned}\right\} \quad \text{at } x^2 + y^2 = \infty \tag{3.5}$$

The shape of the aerofoil can be defined using two functions, one for the upper side of the aerofoil and one for the lower side

$$y = \begin{cases} y_+(t,x) & \text{on the upper side} \\ y_-(t,x) & \text{on the lower side} \end{cases} \tag{3.6}$$

When a particle comes in contact with the aerofoil surface it stays on it for a finite period of time giving

$$x = x(t), \quad y = y(t) \tag{3.7a}$$
$$u = \dot{x}(t), \quad v = \dot{y}(t) \tag{3.7b}$$

along the sides of the aerofoil. Substitution of (3.7a) into (3.6) gives the following relationship on the upper and lower side respectively

$$y(t) = y_\pm(t, x(t))$$

Differentiating with respect to time and using (3.7b) gives

$$v = \frac{\partial y_\pm}{\partial t} + u\frac{\partial y_\pm}{\partial x} \qquad \text{at } y = y_\pm(t,x) \tag{3.8}$$

This is the kinematic condition over the aerofoil. In this analysis it will be assumed that the aerofoil is thin

$$\begin{aligned} y_+(t,x) &= \varepsilon Y_+(t,x) \\ y_-(t,x) &= \varepsilon Y_-(t,x) \end{aligned} \tag{3.9}$$

and that the angle of attack is small

$$\alpha = \varepsilon\alpha_* \tag{3.10}$$

As mentioned above, the unsteady flow will generate a wake after the aerofoil, which in the inviscid case is just a discontinuity line due to a difference in velocity as an effect of the anti-symmetric part of the aerofoil shape. The shape of the discontinuity line in non-dimensional form is defined by the arbitrary function

$$y = \varepsilon\eta(t,x), \tag{3.11}$$

where it is assumed that the perturbation of the line is small. The functions for the aerofoil shape and the discontinuity line is shown in Figure 3.2. Differentiating (3.11) with respect to time gives

$$\frac{dy}{dt} = \varepsilon\left(\frac{\partial\eta}{\partial t} + \frac{\partial\eta}{\partial x}\frac{dx}{dt}\right)$$

When a particle comes in contact with the discontinuity line it stays on it for a finite period of time giving that (3.7) is as well valid on the discontinuity line, and the kinematic condition along the wake is obtained

$$v(t) = \varepsilon\left(\frac{\partial\eta}{\partial t} + u(t)\frac{\partial\eta}{\partial x}\right) \quad \text{at} \quad y = \varepsilon\eta(t,x) \tag{3.12}$$

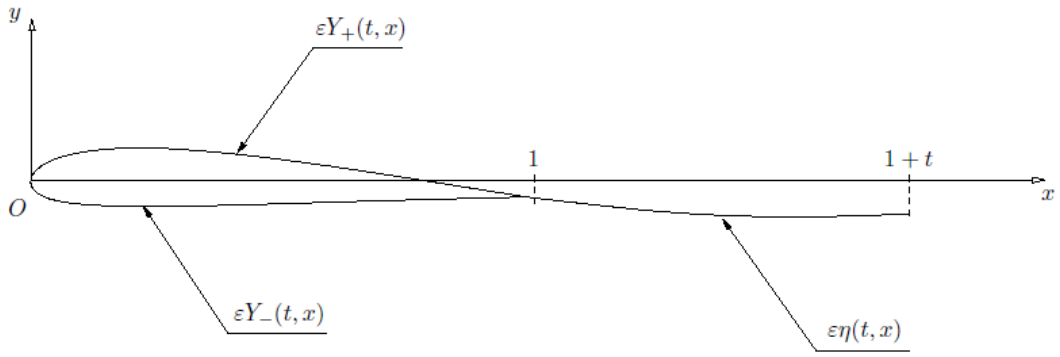

Figure 3.2: Aerofoil assumed thin and the perturbation of the discontinuity line small.

Since the wake is only a discontinuity line the dynamic condition requires that the pressure immediately above the line, p^+, is the same as immediately below, p^-,

$$p\Big|_{y=\eta(t,x)+0} = p\Big|_{y=\eta(t,x)-0} \tag{3.13}$$

The Euler equations (3.4) with the boundary conditions (3.5), the kinematic condition along the sides of the aerofoil (3.8) and along the wake (3.12) as well as the dynamic condition (3.13) states the problem defining the flow field. It is assumed that the aerofoil is thin, the perturbation of the discontinuity line modeling the wake is small, and that the angle of attack is small.

3.2 Linearising

To make the equations easier to solve the above equations will be linearised and terms of order ε^2 will be neglected. When $\varepsilon \to 0$ the aerofoil will become a flat plate which in the inviscid flow field will not cause any perturbation. The unperturbed flow field is as stated above $\hat{u} = U_\infty \cos\alpha$, $\hat{v} = U_\infty \sin\alpha$ and $\hat{p} = p_\infty$. The $\cos\alpha$ and $\sin\alpha$ terms can be expressed in power series expansions [10] according to

$$\begin{aligned} \cos\alpha &= 1 - \frac{\alpha^2}{2!} + \frac{\alpha^4}{4!} - \frac{\alpha^6}{6!} + \ldots = 1 + \mathcal{O}(\varepsilon^2) \\ \sin\alpha &= \alpha - \frac{\alpha^3}{3!} + \frac{\alpha^5}{5!} - \frac{\alpha^7}{7!} + \ldots = \varepsilon\alpha_* + \mathcal{O}(\varepsilon^2) \end{aligned} \tag{3.14}$$

where it has been taken into account that $\alpha = \varepsilon\alpha_*$. This gives that the unperturbed flow field takes the shape of $u = 1$, $v = \varepsilon\alpha_*$ and $p = 0$ in non-dimensional form. A solution in the form of a straight forward asymptotic expansion is therefore tried according to

$$u(t, x, y, \varepsilon) = 1 + \varepsilon u_1(t, x, y) + \ldots \tag{3.15a}$$

$$v(t, x, y, \varepsilon) = \varepsilon\alpha_* + \varepsilon v_1(t, x, y) + \ldots \tag{3.15b}$$

$$p(t, x, y, \varepsilon) = \varepsilon p_1(t, x, y) + \ldots \tag{3.15c}$$

Substituted into (3.4) and neglecting terms of order ε^2 leads to the linearised Euler equations

$$\frac{\partial u_1}{\partial t} + \frac{\partial u_1}{\partial x} = -\frac{\partial p_1}{\partial x} \tag{3.16a}$$

$$\frac{\partial v_1}{\partial t} + \frac{\partial v_1}{\partial x} = -\frac{\partial p_1}{\partial y} \tag{3.16b}$$

$$\frac{\partial u_1}{\partial x} + \frac{\partial v_1}{\partial y} = 0 \tag{3.16c}$$

The boundary conditions (3.5) are linearised by substituting (3.14) into the right hand side of (3.5) and (3.15) into the left hand side, giving

$$\left.\begin{aligned} u_1(t,x,y) &= 0 \\ v_1(t,x,y) &= \alpha_* \\ p_1(t,x,y) &= 0 \end{aligned}\right\} \quad \text{at } x^2+y^2=\infty \tag{3.17}$$

where terms of order ε^2 have been neglected. These are the linearised boundary conditions at infinity.

Substituting (3.15) and (3.9) into (3.8) gives

$$v_1(t,x,y=0\pm) = \frac{\partial Y_\pm(t,x)}{\partial t} + \frac{\partial Y_\pm(t,x)}{\partial x} \tag{3.18}$$

which is the linearised kinematic condition for the aerofoil.

When (3.15) is applied on the discontinuity line, $y = \varepsilon\eta$, the third argument in u_1 and v_1 is small. Taylor expansion of u_1 and v_1 around $y = 0$ gives

$$u_1(t,x,\varepsilon\eta(t,x)) = u_1(t,x,0) + \frac{\partial u_1}{\partial y}(t,x,0)\cdot\varepsilon\eta(t,x) + \mathcal{O}(\varepsilon^2)$$

$$v_1(t,x,\varepsilon\eta(t,x)) = v_1(t,x,0) + \frac{\partial v_1}{\partial y}(t,x,0)\cdot\varepsilon\eta(t,x) + \mathcal{O}(\varepsilon^2)$$

Substitution into (3.15) gives

$$\left.\begin{aligned} u &= 1 + \varepsilon u_1(t,x,0) + \mathcal{O}(\varepsilon^2) \\ v &= \varepsilon v_1(t,x,0) + \mathcal{O}(\varepsilon^2) \end{aligned}\right. \quad \text{at} \quad y = \varepsilon\eta(t,x) \tag{3.19}$$

which in (3.12) gives the linearised kinematic condition for the wake

$$v_1(t,x,y=0) = \frac{\partial \eta(t,x)}{\partial t} + \frac{\partial \eta(t,x)}{\partial x} \tag{3.20}$$

Equation (3.15c) applied just above and below the discontinuity line gives

$$p^+ = \varepsilon p_1^+ + \ldots$$

$$p^- = \varepsilon p_1^- + \ldots$$

which simply gives the dynamic condition (3.13) in linearised form to

$$p_1\Big|_{y=+0} = p_1\Big|_{y=-0} \tag{3.21}$$

The linearised Euler equations (3.16) with (3.17), (3.18), (3.20) and (3.21) now states the linearised boundary and initial value problem defining the flow field around the aerofoil.

3.3 Velocity jump across the discontinuity line

To find an equation for the velocity jump across the wake the linearised dynamic condition (3.21) with the x-momentum equation is used. Applying the linearised x-momentum equation (3.16a) just above and below the discontinuity line gives

$$\frac{\partial u_1^+}{\partial t} + \frac{\partial u_1^+}{\partial x} = -\frac{\partial p_1^+}{\partial x} \tag{3.22a}$$

$$\frac{\partial u_1^-}{\partial t} + \frac{\partial u_1^-}{\partial x} = -\frac{\partial p_1^-}{\partial x} \tag{3.22b}$$

Subtracting (3.22b) from (3.22a) gives

$$\frac{\partial (u_1^+ - u_1^-)}{\partial t} + \frac{\partial (u_1^+ - u_1^-)}{\partial x} = -\frac{\partial (p_1^+ - p_1^-)}{\partial x} \tag{3.23}$$

where the right hand side according to (3.21) is zero. The velocity jump across the discontinuity line is now defined as

$$\gamma = u_1^+ - u_1^- \tag{3.24}$$

Substituted into (3.23) gives a partial differential equation for the velocity jump across the discontinuity line

$$\frac{\partial \gamma}{\partial t} + \frac{\partial \gamma}{\partial x} = 0 \tag{3.25}$$

which is a known differential equation with solution

$$\gamma(t, x) = \Theta(t - x)$$

where $\Theta(\xi)$ is an arbitrary function of ξ. If the initial distribution of the velocity jump is the function $\theta(x)$, then

$$\gamma(0, x) = \Theta(-x) = \theta(x)$$

and it follows that $\Theta(\xi) = \theta(-\xi) = \theta(x - t)$. Hence,

$$\gamma(t, x) = \theta(x - t) \tag{3.26}$$

which shows that the initial velocity jump travels down in the x-direction, so at time t the initial velocity jump will have travelled a distance t, hence will be at the position $1 + t$ in the x-direction.

Chapter 4

Solution in the complex plane

4.1 The Cauchy-Riemann equations

To be able to solve the linearised Euler equations (3.16) the pressure is eliminated as a first step by combining the x- and y-momentum equations. Differentiating (3.16a) with respect to y and (3.16b) with respect to x and subtracting the first from the second leads to

$$\frac{\partial}{\partial t}(\frac{\partial v_1}{\partial x} - \frac{\partial u_1}{\partial y}) + \frac{\partial}{\partial x}(\frac{\partial v_1}{\partial x} - \frac{\partial u_1}{\partial y}) = 0 \tag{4.1}$$

Vorticity in a two-dimensional flow is defined as $\underline{w} = (0, 0, w)$ where

$$w \equiv \frac{\partial v}{\partial x} - \frac{\partial u}{\partial y} \tag{4.2}$$

which in (4.1) gives

$$\frac{\partial w}{\partial t} + \frac{\partial w}{\partial x} = 0$$

which is a partial differential equation for the vorticity in the same form as (3.25). The solution process is therefore the same as above, hence

$$w(t, x) = \Omega(x - t) \tag{4.3}$$

where $\Omega(t, x)$ is the initial distribution for the vorticity and (4.3) states that the initial distribution travels down in the x-direction with time. Initially there is no wake, hence the vorticity distribution is zero. Equation (4.3) therefore states that the function for the vorticity will always be zero. In other words

$$\frac{\partial v_1}{\partial x} - \frac{\partial u_1}{\partial y} = 0$$

The latter equation can be rewritten as

$$\frac{\partial u_1}{\partial y} = -\frac{\partial(-v_1)}{\partial x} \tag{4.4}$$

The continuity equation (3.16c) can be rewritten as

$$\frac{\partial u_1}{\partial x} = \frac{\partial(-v_1)}{\partial y} \tag{4.5}$$

and one can see that together (4.4) and (4.5) are the Cauchy-Riemann equations. This gives that u_1 and $-v_1$ constitute the real and imaginary parts of an analytic function. Here, u_1 is set to be the real part and $-v_1$ is set to be the imaginary part [1] giving

$$f(z) = u_1(x, y) - iv_1(x, y) \tag{4.6}$$

where $f(z)$ is the analytic function. The solution to the linearised Euler equations can therefore be found in the complex plane by finding a function $f(z)$ which is analytic on the entire z-plane except on a branch cut encircling the aerofoil and the wake where the Euler equations do not hold, hence removing all discontinuities. The branch cut is therefore made along $\hat{x} \in [0, c + U_\infty \hat{t}]$ which in non-dimensional form is $x \in [0, 1 + t]$. Furthermore, $f(z)$ must satisfy the kinematic conditions over the aerofoil and the wake as well as the boundary conditions at infinity. In other words, finding the function $f(z)$ such that

1. $f(z)$ is analytic on the entire z-plane except on a branch cut made along the interval $x \in [0, 1 + t]$ on the real axis,

2. its imaginary part on the upper and lower side of the branch cut is

$$\Im\{f(z)\} = \begin{cases} \left.\begin{array}{ll} -(\dfrac{\partial Y_+(t,x)}{\partial t} + \dfrac{\partial Y_+(t,x)}{\partial x}) & \text{at } y = 0+ \\ -(\dfrac{\partial Y_-(t,x)}{\partial t} + \dfrac{\partial Y_-(t,x)}{\partial x}) & \text{at } y = 0- \end{array}\right\} & 0 \le x \le 1 \\ \left.\begin{array}{ll} -(\dfrac{\partial \eta_+(t,x)}{\partial t} + \dfrac{\partial \eta_+(t,x)}{\partial x}) & \text{at } y = 0+ \\ -(\dfrac{\partial \eta_-(t,x)}{\partial t} + \dfrac{\partial \eta_-(t,x)}{\partial x}) & \text{at } y = 0- \end{array}\right\} & 1 < x \le 1 + t \end{cases} \tag{4.7}$$

3. in the far distance $f(z)$ is bounded according to

$$f(z) \to -i\alpha_* \text{ as } z \to \infty \tag{4.8}$$

With the approximation of inviscid flow the momentum equations for the flow reduce in order. Another restriction is needed to make the solution unique, which is the Kutta-condition, stating that the function $f(z)$ is bounded at the trailing edge. The Kutta-condition is mathematically written as

$$f(z) = o\big[(z-1)^{-1/2}\big] \quad \text{as } z \to 1 \tag{4.9}$$

[1] This could have been chosen the other way around as well.

4.2 Cauchy's integral formula

A formula is now derived using Cauchy's integral formula for an arbitrary function $F(z)$ which has the following properties

1. is analytic on the entire z-plane except for maybe on the branch cut made along $x \in [0, 1+t]$ on the real axis,

2. has a finite limit at infinity

$$F(z) \to a \text{ as } z \to \infty \tag{4.10}$$

3. near the leading edge, trailing edge and at the end of the wake satisfies the following restrictions

$$F(z) = o(z^{-1}) \text{ as } z \to 0 \tag{4.11a}$$
$$F(z) = o\big[(z-1)^{-1}\big] \text{ as } z \to 1 \tag{4.11b}$$
$$F(z) = o\big[\big(z-(1+t)\big)^{-1}\big] \text{ as } z \to 1+t \tag{4.11c}$$

Applying Cauchy's integral formula to $F(z)$ gives

$$F(z) = \frac{1}{2\pi i} \int_C \frac{F(\zeta)}{\zeta - z} d\zeta \tag{4.12}$$

This is a line integration along the contour C, valid for any arbitrary function $F(z)$ which is analytic on and inside C.
The integration is taken along the contour C which is composed of $C_R, C_r, C_u, C_l, C_r', C_{a+}$, C_{a-}, C_{w+} and C_{w-} according to Figure 4.1, where the direction of integration is shown in the figure. The outer integration is taken along C_R which is a circle of radius R, centred at $z = 0$, where R is taken large enough so that the point z and the branch cut are inside C_R. Together $C_r, C_u, C_l, C_r', C_{a+}, C_{a-}, C_{w+}$ and C_{w-} encircle the branch cut, hence removing the parts with discontinuities where the analytic formulas do not hold. The small circles are placed over possible singularities, hence placed with the centers at the leading and trailing edges as well as at the end of the wake, all with radius r.

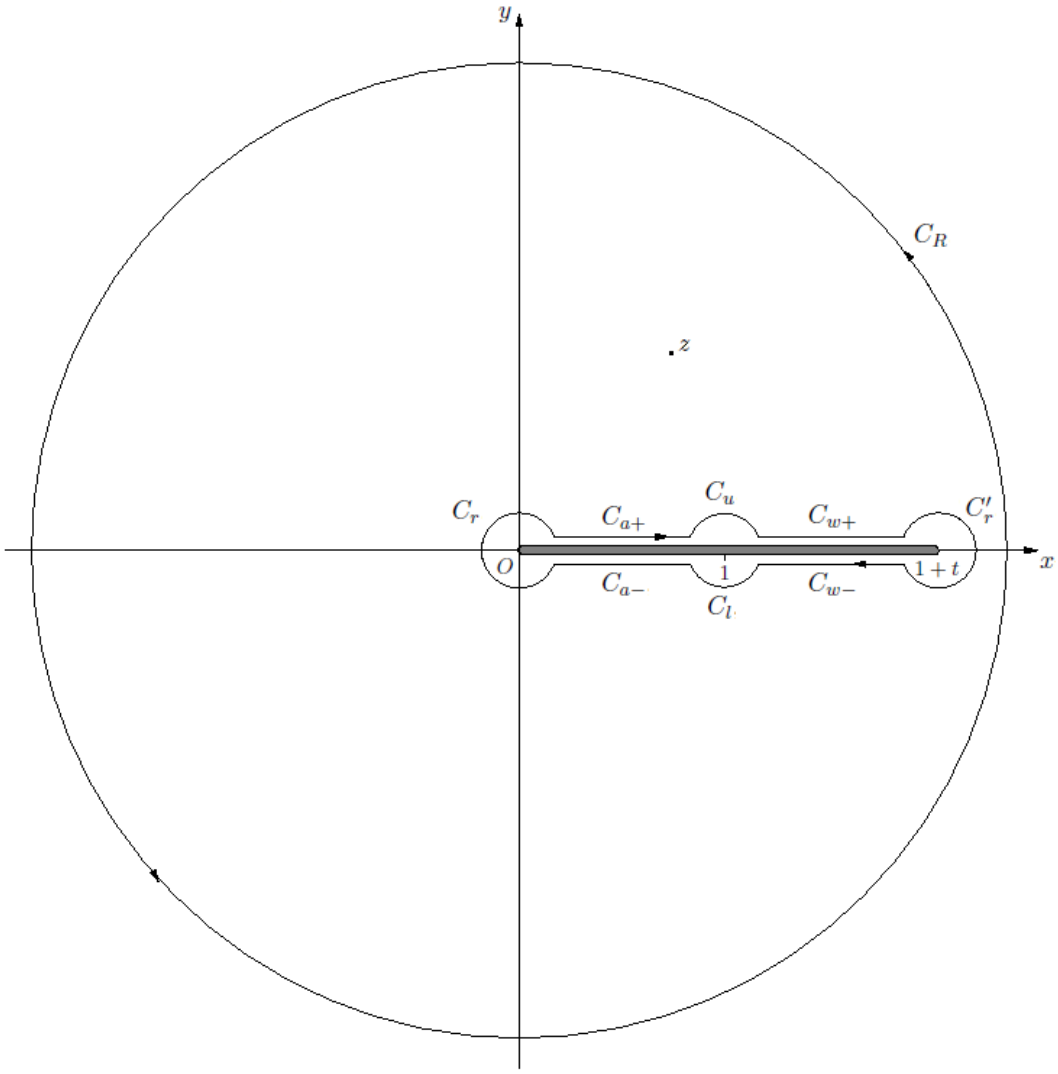

Figure 4.1: The contour of integration C.

Accordingly, the integration in (4.12) can be decomposed as

$$F(z) = \frac{1}{2\pi i}\left\{\int_{C_R} + \int_{C_r} + \int_{C_u} + \int_{C_l} + \int_{C'_r} + \int_{C_{a+}} + \int_{C_{a-}} + \int_{C_{w+}} + \int_{C_{w-}}\right\} \frac{F(\zeta)}{\zeta - z}\, d\zeta \tag{4.13}$$

The integration around C_R is evaluated first. Since the size of R only is restricted from below it can be taken large enough so that $F(\zeta) \to a$ according to (4.10), hence

$$\frac{1}{2\pi i}\int_{C_R} \frac{F(\zeta)}{\zeta - z} d\zeta = \frac{1}{2\pi i}\int_{C_R} \frac{a + \text{h.o.t.}}{\zeta - z} d\zeta \tag{4.14}$$

and since ζ is large

$$\frac{1}{\zeta - z} = \frac{1}{\zeta}\frac{1}{1 - z/\zeta} = \frac{1}{\zeta}\big(1 + \frac{z}{\zeta} + ...\big) = \frac{1}{\zeta} + \mathcal{O}(\frac{1}{\zeta^2})$$

which substituted into (4.14) and neglecting $\mathcal{O}(1/\zeta^2)$ terms gives

$$\frac{1}{2\pi i}\int\limits_{C_R} \frac{F(\zeta)}{\zeta - z} d\zeta = \frac{a}{2\pi i}\int\limits_{C_R} \frac{1}{\zeta} d\zeta \tag{4.15}$$

When ζ is on C_R it can be represented in polar coordinates $\zeta = Re^{i\nu}$ where ν is the angle which decreases from 0 to 2π and $d\zeta = iRe^{i\nu}d\nu$, which in (4.15) gives

$$\frac{1}{2\pi i}\int\limits_{C_R} \frac{F(\zeta)}{\zeta - z} d\zeta = \frac{a}{2\pi i}\int\limits_{0}^{2\pi} \frac{1}{Re^{i\nu}} iRe^{i\nu} d\nu = \frac{a}{2\pi i}\int\limits_{0}^{2\pi} i d\nu = a \tag{4.16}$$

The integrals around the small circles will now be investigated. It will be shown that these integrals vanish as their radius goes to zero, i.e. when the circles shrink to a point. It can be shown that they are all bounded by an upper limit;

$$\left|\frac{1}{2\pi i}\int\limits_{C_0} \frac{F(\zeta)}{\zeta - z} d\zeta\right| \leq \frac{1}{2\pi}\int\limits_{C_0} \frac{|F(\zeta)|}{|\zeta - z|} |d\zeta|$$

where C_0 can be either of C_r, C_u, C_l or C_r'. Using the fact that ζ is on C_0 and z is outside C_0 gives

$$|\zeta - z| \geq |z| - |\zeta| = |z| - r$$

which gives

$$\left|\frac{1}{2\pi i}\int\limits_{C_0} \frac{F(\zeta)}{\zeta - z} d\zeta\right| \leq \frac{1}{2\pi(|z| - r)}\int\limits_{C_0} |F(\zeta)||d\zeta| \tag{4.17}$$

Representing ζ in polar coordinates on C_0 if the centre of C_0 is placed arbitrary on the real axis at x_0

$$\zeta = x_0 + re^{i\nu} \quad \Rightarrow |d\zeta| = rd\nu$$

with the angle changing from ν_1 to ν_2 along C_0. Substituted into (4.17) finally gives

$$\left|\frac{1}{2\pi i}\int\limits_{C_0} \frac{F(\zeta)}{\zeta - z} d\zeta\right| \leq \frac{1}{2\pi(|z| - r)}\int\limits_{\nu_1}^{\nu_2} |F(\zeta)| r d\nu \tag{4.18}$$

Now the four specific cases C_r, C_u, C_l and C_r' are investigated;

Along C_r:

$$\zeta = re^{i\nu}, \qquad \nu \text{ goes from } 2\pi \text{ to } 0$$

As $r \to 0 \Rightarrow \zeta \to 0$ and (4.11a) gives

$$F(\zeta) = \beta \cdot 1/\zeta \Rightarrow |F(\zeta)| = \beta \cdot 1/r$$

where β by definition $\to 0$. Hence, $|F(\zeta)|r \to 0$ and the integral on the right hand side in (4.18) vanishes.

Along C_u and C_l:

$$\zeta = 1 + re^{i\nu}, \qquad \nu \text{ goes from } \pi \text{ to } 0$$
$$\zeta = 1 + re^{i\nu}, \qquad \nu \text{ goes from } 2\pi \text{ to } \pi$$

respectively. As $r \to 0 \Rightarrow \zeta \to 1$ and (4.11b) gives

$$F(\zeta) = \beta \frac{1}{\zeta - 1} = \beta \frac{1}{1 + re^{i\nu} - 1} \Rightarrow |F(\zeta)| = \beta \frac{1}{r}$$

Hence, $|F(\zeta)|r \to 0$ and the integral on the right hand side in (4.18) vanishes.

Along C_r':

$$\zeta = 1 + t + re^{i\nu}, \qquad \nu \text{ goes from } \pi \text{ to } -\pi$$

As $r \to 0 \Rightarrow \zeta \to 1 + t$ and (4.11c) gives

$$F(\zeta) = \beta \frac{1}{\zeta - (1+t)} = \beta \frac{1}{1 + t + re^{i\nu} - (1+t)} \Rightarrow |F(\zeta)| = \beta \frac{1}{r}$$

Hence, $|F(\zeta)|r \to 0$ and the integral on the right hand side in (4.18) vanishes.

This together with (4.16) makes (4.13) reduce to

$$F(z) = a + \frac{1}{2\pi i}\left(\int\limits_{C_{a+}} \frac{F(\zeta)}{\zeta - z}\, d\zeta + \int\limits_{C_{a-}} \frac{F(\zeta)}{\zeta - z}\, d\zeta + \int\limits_{C_{w+}} \frac{F(\zeta)}{\zeta - z}\, d\zeta \int\limits_{C_{w-}} \frac{F(\zeta)}{\zeta - z}\, d\zeta \right) \tag{4.20}$$

The integration along C_{a+} is from 0 to 1 and along C_{a-} is from 1 to 0. The integration along C_{w+} is from 1 to $1 + t$ and along C_{w-} is from $1 + t$ to 1. Changing direction of integration in two of the integrals and denoting $F(z)$ on the upper and lower side of the branch cut by $F^+(x)$ and $F^-(x)$ respectively gives that (4.20) can be written as

$$F(z) = a + \frac{1}{2\pi i} \int\limits_0^1 \frac{F^+(\zeta) - F^-(\zeta)}{\zeta - z}\, d\zeta + \frac{1}{2\pi i} \int\limits_1^{1+t} \frac{F^+(\zeta) - F^-(\zeta)}{\zeta - z}\, d\zeta \tag{4.21}$$

4.3 Looking at the anti-symmetric part of the flow

The function $f(z)$ representing the flow, equation (4.6), can be subdivided into a sum of two functions, f_1 and f_2, one for the flow around the symmetric part of the aerofoil and one for the flow around the anti-symmetric part. These are analytic on the entire z-plane except on the branch cut and will be sought in the class of functions satisfying the Kutta condition (4.9).

$$f(z) = f_1(z) + f_2(z) \tag{4.22}$$

The boundary conditions for the two parts are set to be

Symmetric part:

$$\Im\{f_1(z)\} = \begin{cases} v^{(1)}(x) & \text{at } y = 0+ \\ -v^{(1)}(x) & \text{at } y = 0- \end{cases} \tag{4.23}$$

$$f_1(z) \to 0 \quad \text{as } z \to \infty \tag{4.24}$$

Anti-symmetric part:

$$\Im\{f_2(z)\} = \begin{cases} v^{(2)}(x) & \text{at } y = 0+ \\ v^{(2)}(x) & \text{at } y = 0- \end{cases} \tag{4.25}$$

$$f_2(z) \to -i\alpha_* \quad \text{as } z \to \infty \tag{4.26}$$

Since f_1 and f_2 are analytic functions, so is their sum $f(z)$. The freestream condition (4.8) is satisfied by (4.24) and (4.26). To satisfy the kinematic condition (4.7) using (4.23) and (4.25) the following equations for $v^{(1)}$ and $v^{(2)}$ are obtained

In the region $0 \le x \le 1$:

$$-\frac{\partial Y_+}{\partial t} - \frac{\partial Y_+}{\partial x} = v^{(1)} + v^{(2)} \tag{4.27a}$$

$$-\frac{\partial Y_-}{\partial t} - \frac{\partial Y_-}{\partial x} = -v^{(1)} + v^{(2)} \tag{4.27b}$$

In the region $1 \le x \le 1 + t$:

$$-\frac{\partial \eta_+}{\partial t} - \frac{\partial \eta_+}{\partial x} = v^{(1)} + v^{(2)} \tag{4.28a}$$

$$-\frac{\partial \eta_-}{\partial t} - \frac{\partial \eta_-}{\partial x} = -v^{(1)} + v^{(2)} \tag{4.28b}$$

Solving for $v^{(1)}$ and $v^{(2)}$ in both regions gives

$$\left.\begin{aligned} v^{(1)} &= -\frac{1}{2}\left[\frac{\partial}{\partial t}(Y_+ - Y_-) + \frac{\partial}{\partial x}(Y_+ - Y_-)\right] \\ v^{(2)} &= -\frac{1}{2}\left[\frac{\partial}{\partial t}(Y_+ + Y_-) + \frac{\partial}{\partial x}(Y_+ + Y_-)\right] \end{aligned}\right\} \quad \text{at } 0 \le x \le 1 \tag{4.29}$$

$$\left.\begin{aligned} v^{(1)} &= -\frac{1}{2}\left[\frac{\partial}{\partial t}(\eta_+ - \eta_-) + \frac{\partial}{\partial x}(\eta_+ - \eta_-)\right] \\ v^{(2)} &= -\frac{1}{2}\left[\frac{\partial}{\partial t}(\eta_+ + \eta_-) + \frac{\partial}{\partial x}(\eta_+ + \eta_-)\right] \end{aligned}\right\} \quad \text{at } 1 \leq x \leq 1+t \tag{4.30}$$

A flow around a symmetric aerofoil does not generate a wake, the wake is only due to the difference in surface shape of the upper and lower side of the aerofoil, hence only due to the anti-symmetric part of the aerofoil. Further a symmetric aerofoil does not contribute to the lift force, only drag. Since the aim is to find a function for the velocity jump across the wake as well as investigating flutter, which is not affected by drag, only lift, the symmetric part $f_1(z)$ will neither contribute to the wake nor flutter and only the anti-symmetric part will be studied further on. Applying (4.21) to the anti-symmetric part gives

$$f_2(z) = -i\alpha_* + \frac{1}{2\pi i}\int_0^1 \frac{f_2^+(\zeta) - f_2^-(\zeta)}{\zeta - z}\,d\zeta + \frac{1}{2\pi i}\int_1^{1+t} \frac{f_2^+(\zeta) - f_2^-(\zeta)}{\zeta - z}\,d\zeta$$

Equation (4.25) states that $\Im\{f_2^+\} = \Im\{f_2^-\} \Rightarrow f_2^+ - f_2^- = \Re\{f_2^+\} - \Re\{f_2^-\}$ which substituted into the equation above gives

$$\begin{aligned} f_2(z) = -i\alpha_* &+ \frac{1}{2\pi i}\int_0^1 \frac{\Re\{f_2^+(\zeta)\} - \Re\{f_2^-(\zeta)\}}{\zeta - z}\,d\zeta + \\ &+ \frac{1}{2\pi i}\int_1^{1+t} \frac{\Re\{f_2^+(\zeta)\} - \Re\{f_2^-(\zeta)\}}{\zeta - z}\,d\zeta \end{aligned} \tag{4.31}$$

Applying (4.31) to the conjugate of z gives

$$f_2(\bar{z}) = -i\alpha_* + \frac{1}{2\pi i}\int_0^1 \frac{\Re\{f_2^+(\zeta)\} - \Re\{f_2^-(\zeta)\}}{\zeta - \bar{z}}\,d\zeta + \frac{1}{2\pi i}\int_1^{1+t} \frac{\Re\{f_2^+(\zeta)\} - \Re\{f_2^-(\zeta)\}}{\zeta - \bar{z}}\,d\zeta$$

Taking complex conjugates on both sides gives

$$\overline{f_2(\bar{z})} = i\alpha_* - \frac{1}{2\pi i}\int_0^1 \frac{\Re\{f_2^+(\zeta)\} - \Re\{f_2^-(\zeta)\}}{\zeta - z}\,d\zeta - \frac{1}{2\pi i}\int_1^{1+t} \frac{\Re\{f_2^+(\zeta)\} - \Re\{f_2^-(\zeta)\}}{\zeta - z}\,d\zeta \tag{4.32}$$

By comparing (4.32) to (4.31) one can see that

$$\overline{f_2(\bar{z})} = -f_2(z)$$

which gives

$$\overline{f_2\Big|_{(x,-y)}} = -f_2\Big|_{(x,y)} \quad \Rightarrow \quad \begin{cases} \Re\{f_2\}\Big|_{(x,-y)} = -\Re\{f_2\}\Big|_{(x,y)} \\ \Im\{f_2\}\Big|_{(x,-y)} = \Im\{f_2\}\Big|_{(x,y)} \end{cases} \tag{4.33}$$

This shows that the real part of the function, i.e. u_1, is anti-symmetric around the x-axis, whereas the imaginary part, i.e. $-v_1$, is symmetric around the x-axis. Applying (4.33) to the upper and lower sides of the branch cut gives

$$\Re\{f_2^-(z)\} = -\Re\{f_2^+(z)\} \tag{4.34a}$$
$$\Im\{f_2^-(z)\} = \Im\{f_2^+(z)\} \tag{4.34b}$$

The latter is already stated in (4.25).

Going back to (4.31), in region $1 \leq x \leq 1+t$, $\Re\{f_2^+\} - \Re\{f_2^-\} = u^+ - u^-$ since the contribution to the velocity jump from the symmetric part of the solution is zero. Equation (3.24) therefore gives that $\Re\{f_2^+\} - \Re\{f_2^-\} = \gamma(t,x)$. In region $0 \leq x \leq 1$ the real part of f_2 is not known but the imaginary part is through the kinematic condition (4.25) and (4.29). By using an auxiliary function, $g(z)$, the real part in the expression can be replaced by the imaginary part. This is done by applying (4.21) to the function $F(z) = g(z)f_2(z)$ instead, and is shown below.

4.3.1 Replacing the real parts by imaginary parts by the use of an auxiliary function

The auxiliary function is defined as

$$g(z) = \sqrt{\frac{z}{z-1}} \tag{4.35}$$

where an analytic single-valued branch of it is used according to

$$z = r_1 e^{i\nu_1} \qquad z-1 = r_2 e^{i\nu_2} \quad \Rightarrow \quad g(z) = \sqrt{\frac{r_1}{r_2}} e^{i(\nu_1-\nu_2)/2} \tag{4.36}$$

where the notations in Figure 4.2 have been used. In the far field

$$g(z) \to 1 \text{ as } z \to \infty$$

which with (4.26) gives that

$$f_2(z)g(z) \to -i\alpha_* \text{ as } z \to \infty \tag{4.37}$$

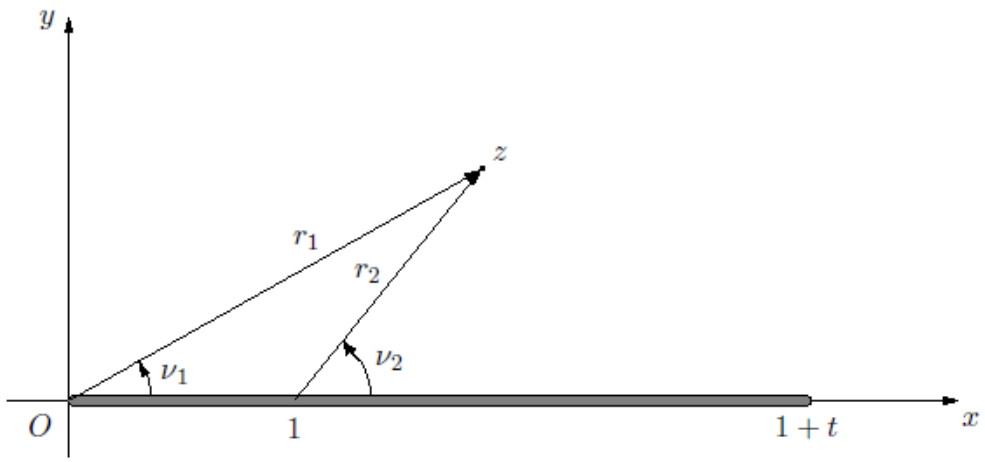

Figure 4.2: Expressing z in polar coordinates.

It is now investigated what form $g(z)$ takes on the upper and lower sides of the branch cut.

In region $0 \leq x \leq 1$**:**

At any point immediately above or below the cut in this region

$$r_1 = x, \quad r_2 = 1 - x \tag{4.38}$$

Reaching the upper side of the cut according to Figure 4.3, path (1) gives the angles to

$$v_1 = 0, \quad v_2 = \pi \tag{4.39}$$

Reaching the lower side of the cut according to Figure 4.3 gives the angles to

$$v_1 = 2\pi, \quad v_2 = \pi \qquad \text{by path (2)} \tag{4.40a}$$

$$v_1 = 0, \quad v_2 = -\pi \qquad \text{by path (3)} \tag{4.40b}$$

where the path cannot cross the branch cut. Either path can be chosen, another example is path (4) showed in Figure 4.4, the only difference is that both ν_1 and ν_2 will increase with a factor $2\pi n$ where $n = 0, \pm 1, \pm 2, \cdots$ is the number of laps. When ν_1 and ν_2 are substituted into (4.36) this extra term will cancel out since both angles increase or decrease equally much, which is also showed below when calculating $g(z)$. Substituting (4.38) and (4.39) into (4.36) gives $g(z)$ on the upper side to

$$g^+(x) = \sqrt{\frac{x}{1-x}} e^{i(0-\pi)/2} = -i\sqrt{\frac{x}{1-x}} \qquad \text{at } 0 \leq x \leq 1 \tag{4.41}$$

and (4.38) and (4.44) into (4.36) gives $g(z)$ on the lower side to

$$g^-(x) = \sqrt{\frac{x}{1-x}} e^{i(0+\pi)/2} = \sqrt{\frac{x}{1-x}} e^{i(2\pi-\pi)/2} = i\sqrt{\frac{x}{1-x}} \qquad \text{at } 0 \leq x \leq 1 \tag{4.42}$$

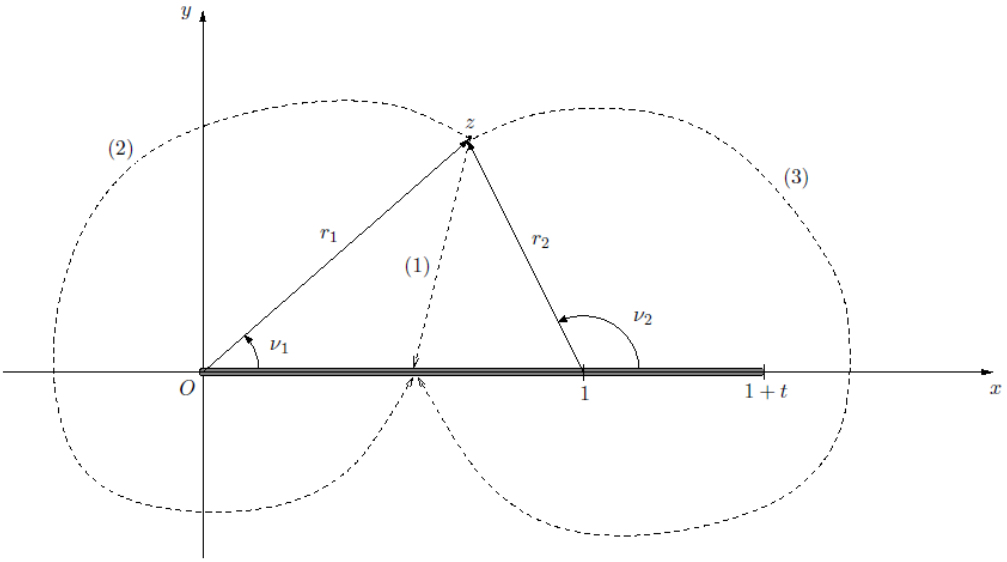

Figure 4.3: Illustration of how a point on the upper side is reached as well as two possible paths to reach a point on the lower side.

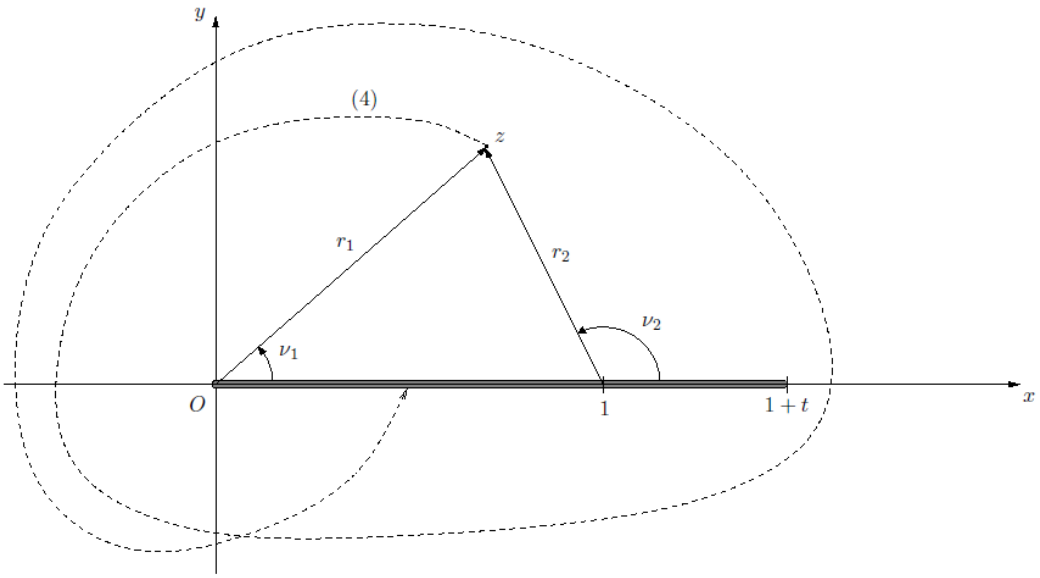

Figure 4.4: A third way of reaching a point on the lower side.

In region $1 \leq x \leq 1+t$:

At any point immediately above or below the cut in this region

$$r_1 = x, \quad r_2 = x - 1 \tag{4.43}$$

Reaching the upper and lower side of the cut in the way showed in Figure 4.5 gives the angles to

$$v_1 = 0, \quad v_2 = 0 \qquad \text{upper side} \tag{4.44a}$$

$$v_1 = 0, \quad v_2 = 0 \qquad \text{lower side} \tag{4.44b}$$

Substituting (4.43) and (4.44a) into (4.36) gives $g(z)$ on the upper side to

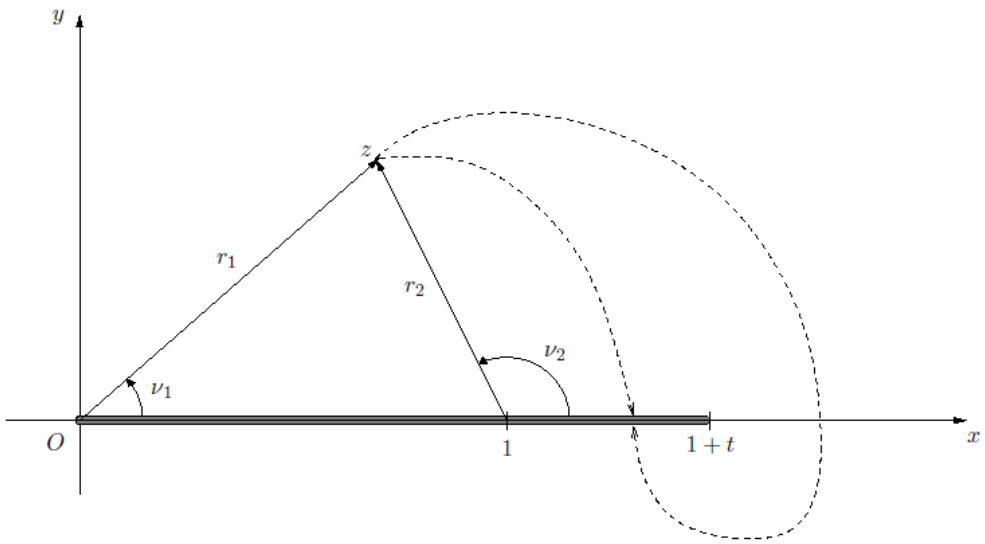

Figure 4.5: Illustration of the paths chosen to reach a point on the upper and lower side.

$$g^+(x) = \sqrt{\frac{x}{x-1}}e^{i\cdot 0} = \sqrt{\frac{x}{x-1}} \qquad \text{at } 1 \le x \le 1+t \tag{4.45}$$

and (4.43) and (4.44b) into (4.36) gives $g(z)$ on the lower side to

$$g^-(x) = \sqrt{\frac{x}{x-1}}e^{i\cdot 0} = \sqrt{\frac{x}{x-1}} \qquad \text{at } 1 \le x \le 1+t \tag{4.46}$$

Now, applying (4.21) to $F(z) = f_2(z)g(z)$ and using (4.37) gives

$$F(z) = -i\alpha_* + \frac{1}{2\pi i}\int_0^1 \frac{F^+(\zeta) - F^-(\zeta)}{\zeta - z}\,d\zeta + \frac{1}{2\pi i}\int_1^{1+t} \frac{F^+(\zeta) - F^-(\zeta)}{\zeta - z}\,d\zeta \tag{4.47}$$

In region $0 \leq \zeta \leq 1$**:**

$$\begin{aligned} F^+(\zeta) - F^-(\zeta) &= g^+(\zeta) f_2^+(\zeta) - g^-(\zeta) f_2^-(\zeta) = \\ &= -i\sqrt{\frac{\zeta}{1-\zeta}} f_2^+(\zeta) - i\sqrt{\frac{\zeta}{1-\zeta}} f_2^-(\zeta) = \\ &= -i\sqrt{\frac{\zeta}{1-\zeta}} (f_2^+(\zeta) + f_2^-(\zeta)) \end{aligned}$$

where (4.41) and (4.42) have been used. Equation (4.34a) and (4.34b) further give that

$$f_2^+(\zeta) + f_2^-(\zeta) = \Re\{f_2^+\} + \Re\{f_2^-\} + i\big(\Im\{f_2^+\} + \Im\{f_2^-\}\big) = 2i\Im\{f_2^+\}$$

hence

$$F^+(\zeta) - F^-(\zeta) = 2\sqrt{\frac{\zeta}{1-\zeta}}\Im\{f_2^+\} \tag{4.48}$$

In region $1 \leq \zeta \leq 1 + t$**:**

$$\begin{aligned} F^+(\zeta) - F^-(\zeta) &= g^+(\zeta) f_2^+(\zeta) - g^-(\zeta) f_2^-(\zeta) = \\ &= \sqrt{\frac{\zeta}{\zeta-1}} f_2^+(\zeta) - \sqrt{\frac{\zeta}{\zeta-1}} f_2^-(\zeta) = \\ &= -\sqrt{\frac{\zeta}{\zeta-1}} (f_2^+(\zeta) - f_2^-(\zeta)) \end{aligned}$$

where (4.45) and (4.46) have been used. Equation (4.34b) gives that

$$f_2^+(\zeta) - f_2^-(\zeta) = \Re\{f_2^+\} - \Re\{f_2^-\} + i\big(\Im\{f_2^+\} - \Im\{f_2^-\}\big) = \Re\{f_2^+\} - \Re\{f_2^-\}$$

hence

$$F^+(\zeta) - F^-(\zeta) = \sqrt{\frac{\zeta}{\zeta-1}}\big(\Re\{f_2^+\} - \Re\{f_2^-\}\big) \tag{4.49}$$

Substitution of (4.48) and (4.49) into (4.47) gives

$$\begin{aligned} F(z) = f_2(z)\sqrt{\frac{z}{z-1}} = -i\alpha_* &+ \frac{1}{2\pi i}\int_0^1 2\sqrt{\frac{\zeta}{1-\zeta}}\frac{\Im\{f_2^+\}}{\zeta - z}\,d\zeta + \\ &+ \frac{1}{2\pi i}\int_1^{1+t}\sqrt{\frac{\zeta}{\zeta-1}}\frac{\Re\{f_2^+\} - \Re\{f_2^-\}}{\zeta - z}\,d\zeta \end{aligned} \tag{4.50}$$

Equations (4.25) and (4.29) give

$$\Im\{f_2^+\} = -\frac{1}{2}\left[\frac{\partial}{\partial t}(Y_+ + Y_-) + \frac{\partial}{\partial \zeta}(Y_+ + Y_-)\right] \tag{4.51}$$

As mentioned above, in the region $1 \leq x \leq 1+t$ we have that $\Re\{f_2^+\} - \Re\{f_2^-\} = u^+ - u^- \equiv \gamma(t,x)$. This together with (4.51) in (4.50) gives

$$f_2(z)\sqrt{\frac{z}{z-1}} = -i\alpha_* - \frac{1}{2\pi i}\int_0^1 \left[\frac{\partial}{\partial t}(Y_+ + Y_-) + \frac{\partial}{\partial \zeta}(Y_+ + Y_-)\right]\sqrt{\frac{\zeta}{1-\zeta}}\frac{1}{\zeta - z}\,d\zeta + \\ + \frac{1}{2\pi i}\int_1^{1+t}\sqrt{\frac{\zeta}{\zeta-1}}\frac{\gamma(t,\zeta)}{\zeta - z}\,d\zeta$$

which when rearranging terms gives an equation for $f_2(z)$ to

$$f_2(z) = \sqrt{\frac{z-1}{z}}\left(- i\alpha_* - \frac{1}{2\pi i}\int_0^1 \left[\frac{\partial}{\partial t}(Y_+ + Y_-) + \frac{\partial}{\partial \zeta}(Y_+ + Y_-)\right]\sqrt{\frac{\zeta}{1-\zeta}}\frac{1}{\zeta - z}\,d\zeta + \right. \\ \left. + \frac{1}{2\pi i}\int_1^{1+t}\sqrt{\frac{\zeta}{\zeta-1}}\frac{\gamma(t,\zeta)}{\zeta - z}\,d\zeta\right) \tag{4.52}$$

4.4 Equation for velocity jump $\gamma(t,x)$

By comparing the expressions for $f_2(z)$ with one where $f_2(z)$ is related to the circulation around the aerofoil an equation for the velocity jump $\gamma(t,x)$ will be achieved. To be able to relate (4.52) to the circulation, the behavior in the far distance is investigated.
For large z and $\zeta \in [0, 1+t]$:

$$\frac{1}{\zeta - z} = -\frac{1}{z}\frac{1}{1-\zeta/z} = -\frac{1}{z}\left(1 + \frac{\zeta}{z} + \left(\frac{\zeta}{z}\right)^2 + \cdots\right) = -\frac{1}{z} + \mathcal{O}\left(\frac{1}{z^2}\right)$$
$$\sqrt{\frac{z-1}{z}} = \sqrt{1 - \frac{1}{z}} = 1 - \frac{1}{2z} + \mathcal{O}\left(\frac{1}{z^2}\right)$$

which substituted into (4.52) gives

$$f_2(z) = (1 - \frac{1}{2z})\left(- i\alpha_* - \frac{1}{2\pi i}\int_0^1 \sqrt{\frac{\zeta}{1-\zeta}}\left[\frac{\partial}{\partial t}(Y_+ + Y_-) + \frac{\partial}{\partial \zeta}(Y_+ + Y_-)\right]\left(- \frac{1}{z}\right)d\zeta \right. \\ \left. - \frac{1}{2\pi i}\int_1^{1+t}\sqrt{\frac{\zeta}{\zeta-1}}\frac{\gamma(t,\zeta)}{z}\,d\zeta\right) + \mathcal{O}\left(\frac{1}{z^2}\right)$$

Neglecting $\mathcal{O}(1/z^2)$ terms gives

$$\begin{aligned} f_2(z) =& -i\alpha_* - \frac{\alpha_*}{2zi} + \frac{1}{2\pi iz}\int_0^1 \sqrt{\frac{\zeta}{1-\zeta}}\left[\frac{\partial}{\partial t}(Y_+ + Y_-) + \frac{\partial}{\partial \zeta}(Y_+ + Y_-)\right] d\zeta \\ & - \frac{1}{2\pi iz}\int_1^{1+t} \sqrt{\frac{\zeta}{\zeta-1}}\gamma(t,\zeta)\, d\zeta = \\ =& -i\alpha_* - \frac{\Gamma_1}{2\pi iz} \end{aligned} \tag{4.53}$$

where

$$\Gamma_1 = \alpha_*\pi - \int_0^1 \sqrt{\frac{\zeta}{1-\zeta}}\left[\frac{\partial}{\partial t}(Y_+ + Y_-) + \frac{\partial}{\partial \zeta}(Y_+ + Y_-)\right] d\zeta + \int_1^{1+t} \sqrt{\frac{\zeta}{\zeta-1}}\gamma(t,\zeta)\, d\zeta \tag{4.54}$$

Since the flow field around an aerofoil placed in a uniform flow can be treated as a superposition of a potential flow and rotational flow, the expression for $f_2(z)$ (4.53) can be compared to an expression for $f_2(z)$ achieved using the complex potential. The complex potential for a vortex in a free stream is in dimensional form

$$w = U_\infty e^{-i\alpha}\hat{z} + \frac{\Gamma}{2\pi i}\ln\hat{z}$$

where Γ is the circulation. Since the flow is investigated in the far distance higher order terms are neglected and for simplicity the vortex is placed at the origin, since the difference in position would be neglected anyway. The complex conjugate velocity is obtained by differentiating with respect to $\hat{z}$ giving

$$\frac{dw}{d\hat{z}} = \hat{u} - i\hat{v} = U_\infty e^{-i\alpha} + \frac{\Gamma}{2\pi i\hat{z}}$$

Non-dimensionalising using (3.3) and $\hat{z} = \hat{x} + i\hat{y} = cx + icy = cz$ gives

$$u - iv = e^{-i\alpha} + \frac{1}{2\pi iz}\frac{\Gamma}{cU_\infty} \tag{4.55}$$

where Γ/cU_∞ is the non-dimensional circulation. The angle of attack is of order ε, $\alpha = \varepsilon\alpha_*$, as stated in (3.10) giving

$$e^{-i\alpha} = e^{-i\varepsilon\alpha_*} = 1 - i\varepsilon\alpha_* + \mathcal{O}(\varepsilon^2) \tag{4.56}$$

Substituting (4.56) and (3.15) into (4.55) gives

$$u_1 - iv_1 = -i\alpha_* + \frac{1}{2\pi iz}\frac{\Gamma}{\varepsilon cU_\infty}$$

Since the left hand side is $f(z)$ and the symmetric part $f_1(z)$ does not contribute to any circulation one have that

$$f_2(z) = -i\alpha_* + \frac{1}{2\pi i z}\frac{\Gamma}{\varepsilon c U_\infty} \tag{4.57}$$

Comparing (4.57) and (4.53) finally gives

$$-i\alpha_* + \frac{1}{2\pi i z}\frac{\Gamma}{\varepsilon c U_\infty} = -i\alpha_* - \frac{\Gamma_1}{2\pi i z}$$

It follows that Γ_1 can be expressed by the circulation Γ according to

$$\Gamma_1 = -\frac{\Gamma}{\varepsilon c U_\infty} \tag{4.58}$$

and one can see that the circulation is of order ε. Equation (4.58) with (4.54) gives

$$\alpha_*\pi - \int_0^1 \sqrt{\frac{\zeta}{1-\zeta}}\left[\frac{\partial}{\partial t}(Y_+ + Y_-) + \frac{\partial}{\partial \zeta}(Y_+ + Y_-)\right] d\zeta + \int_1^{1+t} \sqrt{\frac{\zeta}{\zeta-1}}\gamma(t,\zeta)\, d\zeta = -\frac{\Gamma}{\varepsilon c U_\infty}$$

and rearranging terms leads to

$$\int_1^{1+t} \sqrt{\frac{\zeta}{\zeta-1}}\gamma(t,\zeta)\, d\zeta = \int_0^1 \sqrt{\frac{\zeta}{1-\zeta}}\left[\frac{\partial}{\partial t}(Y_+ + Y_-) + \frac{\partial}{\partial \zeta}(Y_+ + Y_-)\right] d\zeta \; - \; (\alpha_*\pi + \frac{\Gamma}{\varepsilon c U_\infty})$$

where the last term is the initial circulation around an aerofoil. Denoting this to Γ_0 the final equation for γ is written as

$$\int_1^{1+t} \sqrt{\frac{\zeta}{\zeta-1}}\gamma(t,\zeta)\, d\zeta = \int_0^1 \sqrt{\frac{\zeta}{1-\zeta}}\left[\frac{\partial}{\partial t}(Y_+ + Y_-) + \frac{\partial}{\partial \zeta}(Y_+ + Y_-)\right] d\zeta \; - \Gamma_0 \tag{4.59}$$

This is the equation determining the function for the velocity jump $\gamma(t, x)$ in the general case. Solving the integrals on both sides of the equation will give an expression for $\gamma(t, x)$. It will be solved for harmonic oscillations of the aerofoil in the next chapter.

Chapter 5

Harmonic oscillations of aerofoil

The case where the aerofoil performs harmonic oscillations with frequency ω will be studied. In this case the functions for the upper and lower sides of the aerofoil may be written as

$$Y_{\pm}(t,x) = \breve{Y}_{\pm}(x) + \Re\{e^{i\omega t}\widetilde{Y}_{\pm}(x)\} \tag{5.1}$$

where the function for the aerofoil shape has been divided into two parts, one that oscillates, $\widetilde{Y}_{\pm}(x)$, and one that is rigid, $\breve{Y}_{\pm}(x)$. As a response to the aerofoil motion the entire flow field starts to move in an oscillatory movement. This combined with (3.26) gives that the velocity jump at the trailing edge may be sought in the form

$$\gamma(t,x) = \Re\{\gamma_0 e^{i\omega(t-(x-1))}\} = \Re\{\gamma_0 e^{i\omega(t-x+1)}\} \tag{5.2}$$

where the term $x-1$ refers to the fact that the wake does not start until the trailing edge of the aerofoil. The only thing remaining is now to find the amplitude γ_0.
The periodic motion will only have established in the fluid after a long time, hence $t \to \infty$ in the upper limit in the integral on the left hand side of (4.59). However, since

$$\sqrt{\frac{\zeta}{\zeta-1}} \to 1 \text{ as } \zeta \to \infty \tag{5.3}$$

the integral on the left hand side of (4.59) does not converge as $t \to \infty$, and is rewritten as

$$\int_1^{1+t} \sqrt{\frac{\zeta}{\zeta-1}}\gamma(t,\zeta)\,d\zeta = \int_1^{1+t} \gamma(t,\zeta)\,d\zeta + \int_1^{1+t} \left(\sqrt{\frac{\zeta}{\zeta-1}} - 1\right)\gamma(t,\zeta)\,d\zeta$$

Substituting (5.2) into the right hand side of this equation gives

$$\int_1^{1+t} \sqrt{\frac{\zeta}{\zeta-1}}\gamma(t,\zeta)\,d\zeta =$$

$$= \Re\Big\{\gamma_0 e^{i\omega(t+1)} \int_1^{1+t} e^{-i\omega\zeta}\,d\zeta\Big\} + \Re\Big\{\gamma_0 e^{i\omega(t+1)} \int_1^{1+t} \Big(\sqrt{\frac{\zeta}{\zeta-1}} - 1\Big) e^{-i\omega\zeta}\,d\zeta\Big\} =$$

$$= \Re\Big\{\frac{i\gamma_0}{\omega}(1-e^{i\omega t})\Big\} + \Re\Big\{\gamma_0 e^{i\omega(t+1)} \int_1^{1+t} \Big(\sqrt{\frac{\zeta}{\zeta-1}} - 1\Big) e^{-i\omega\zeta}\,d\zeta\Big\}$$

The integral on the right hand side of this equation converges as $t \to \infty$ giving

$$\int_1^{1+t} \sqrt{\frac{\zeta}{\zeta-1}}\gamma(t,\zeta)\,d\zeta =$$

$$= \Re\Big\{\frac{i\gamma_0}{\omega}(1-e^{i\omega t})\Big\} + \Re\Big\{\gamma_0 e^{i\omega(t+1)} \int_1^{\infty} \Big(\sqrt{\frac{\zeta}{\zeta-1}} - 1\Big) e^{-i\omega\zeta}\,d\zeta\Big\} + \cdots \text{ as } t\to\infty =$$

$$= \Re\Big\{\frac{i\gamma_0}{\omega}\Big\} + \Re\Big\{\gamma_0 e^{i\omega t}\Big[e^{i\omega} \int_1^{\infty} \Big(\sqrt{\frac{\zeta}{\zeta-1}} - 1\Big) e^{-i\omega\zeta}\,d\zeta - \frac{i}{\omega}\Big]\Big\} + \cdots \text{ as } t\to\infty \qquad (5.4)$$

Now looking at the right hans side of (4.59), substituting (5.1) into it gives

$$\int_0^1 \sqrt{\frac{\zeta}{1-\zeta}}\Big[\frac{\partial}{\partial t}(Y_+ + Y_-) + \frac{\partial}{\partial\zeta}(Y_+ + Y_-)\Big]\,d\zeta\ - \Gamma_0 =$$

$$\int_0^1 \sqrt{\frac{\zeta}{1-\zeta}}\Big[\breve{Y}'_+(\zeta) + \breve{Y}'_-(\zeta)\Big]\,d\zeta\ - \Gamma_0 +$$

$$+ \Re\Big\{e^{i\omega t} \int_0^1 \sqrt{\frac{\zeta}{1-\zeta}}\Big[i\omega\Big(\widetilde{Y}_+(\zeta) + \widetilde{Y}_-(\zeta)\Big) + \frac{d}{d\zeta}\Big(\widetilde{Y}_+(\zeta) + \widetilde{Y}_-(\zeta)\Big)\Big]\,d\zeta\Big\} \qquad (5.5)$$

Comparing (5.4) and (5.5) the $e^{i\omega t}$ terms must be equal giving

$$\gamma_0 = \frac{1}{D(\omega)} \int_0^1 \sqrt{\frac{\zeta}{1-\zeta}}\Big[i\omega\Big(\widetilde{Y}_+ + \widetilde{Y}_-\Big) + \frac{d}{d\zeta}\Big(\widetilde{Y}_+ + \widetilde{Y}_-\Big)\Big]\,d\zeta \qquad (5.6)$$

where

$$D(\omega) = e^{i\omega} \int_1^{\infty} \Big(\sqrt{\frac{\zeta}{\zeta-1}} - 1\Big) e^{-i\omega\zeta}\,d\zeta - \frac{i}{\omega} \qquad (5.7)$$

is a function of ω only, hence only depends on the frequency of the oscillations and not on the aerofoil shape. It has been calculated numerically and its real and imaginary parts are shown as a function of ω in Figure 5.1.

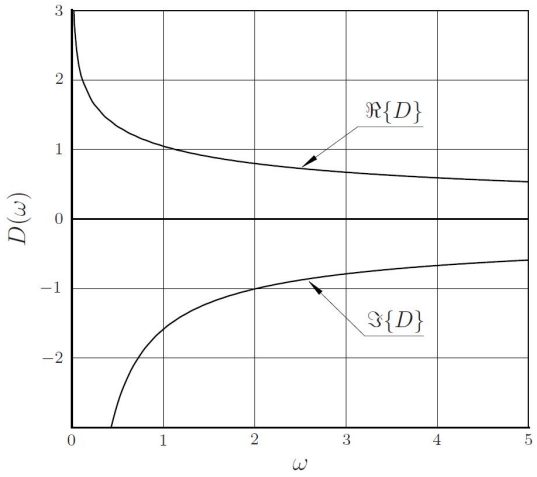

Figure 5.1: Real and imaginary parts of function $D(\omega)$.

To sum up, for harmonic oscillations the function for the velocity jump across the discontinuity line is given by (5.2) where the amplitude of the oscillations is given by (5.6) with (5.7) or Figure 5.1. In the next chapter three different types of oscillations for a symmetric aerofoil will be shown and γ_0 will be evaluated for these cases.

Chapter 6

Application of $\gamma(t, x)$ to a symmetric aerofoil

Now three types of oscillations for a symmetric aerofoil will be investigated; twisting oscillations around a point on the aerofoil, i.e. around the stiffness centre, vertical oscillations and aileron flutter. These cases are the only ones needed to be investigated since the equations are linear and one can use superposition of these three cases to achieve a general one.

As seen in (5.6), to be able to determine the amplitude of the oscillations only $\widetilde{Y}_+ + \widetilde{Y}_-$ is needed, hence only the part of the function determining the shape of the upper and lower side of the aerofoil that is subjected to a deflection.

For a symmetric aerofoil the contribution from the upper side will cancel out with the contribution from the lower side due to the summation. When determining γ_0 the case of symmetric aerofoil will therefore be the same as for a flat plate.

6.1 Twisting oscillation

For the case of twisting oscillations around a point $x_0 \in [0, 1]$ one have

$$\widetilde{Y}_+(x) + \widetilde{Y}_-(x) = -2\alpha_*(x - x_0)$$
$$\frac{d}{dx}(\widetilde{Y}_+(x) + \widetilde{Y}_-(x)) = -2\alpha_*$$

where in the case of a symmetric aerofoil arched parts have canceled out. Figure 6.1 illustrates the oscillations. Substituted into the integral in (5.6) yields

$$\int_0^1 \sqrt{\frac{\zeta}{1-\zeta}}\Big[i\omega\Big(\widetilde{Y}_+ + \widetilde{Y}_-\Big) + \frac{d}{d\zeta}\Big(\widetilde{Y}_+ + \widetilde{Y}_-\Big)\Big]\, d\zeta = \int_0^1 \sqrt{\frac{\zeta}{1-\zeta}}\Big[- 2\alpha_* i\omega\Big(\zeta - \zeta_0) - 2\alpha_*\Big]\, d\zeta$$

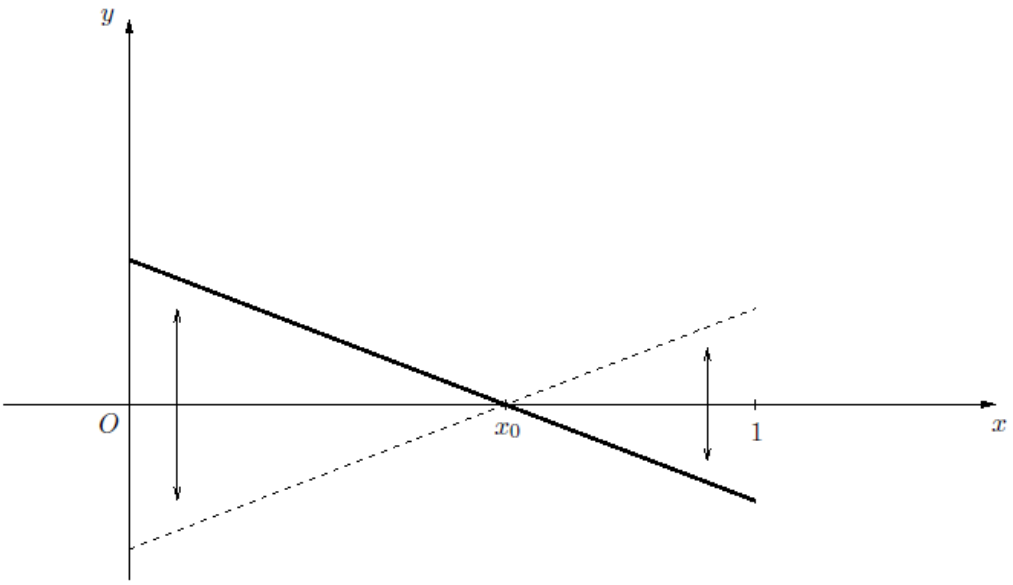

Figure 6.1: Twisting oscillation around a point x_0.

To be able to solve this integral the substitution $\zeta = \sin^2 u$ is used. Change of variable in the integral gives

$$\int_0^1 \sqrt{\frac{\zeta}{1-\zeta}}\Big[-2\alpha_* i\omega\Big(\zeta - \zeta_0) - 2\alpha_*\Big] d\zeta =$$

$$= \int_{n\pi}^{\pi/2+n\pi} 2\sin^2 u\Big(-2\alpha_* i\omega(\sin^2 u - \zeta_0) - 2\alpha_*\Big) du =$$

$$= -4\alpha_* i\omega \int_{n\pi}^{\pi/2+n\pi} \sin^4 u du + 4\alpha_*(i\omega\zeta_0 - 1) \int_{n\pi}^{\pi/2+n\pi} \sin^2 u du \qquad (6.2)$$

The solution to the first integral can easily be found in mathematical handbooks and is [11]

$$\int \sin^4 u du = \frac{3u}{8} - \frac{\sin 2u}{4} + \frac{\sin 4u}{32} \qquad (6.3)$$

For the second integral it is used that $\sin^2 u = 1/2(1 - \cos 2u)$, giving

$$\int \sin^2 u du = \frac{1}{2}\Big(u - \frac{1}{2}\sin 2u\Big) \qquad (6.4)$$

Substituting (6.3) and (6.4) into (6.2) gives

$$\int_0^1 \sqrt{\frac{\zeta}{1-\zeta}}\Big[-2\alpha_* i\omega\Big(\zeta-\zeta_0)-2\alpha_*\Big]\,d\zeta =$$
$$= -4\alpha_* i\omega\Big[\frac{3u}{8}-\frac{\sin 2u}{4}+\frac{\sin 4u}{32}\Big]_{n\pi}^{\pi/2+n\pi} + 2\alpha_*(i\omega\zeta_0-1)\Big[u-\frac{1}{2}\sin 2u\Big]_{n\pi}^{\pi/2+n\pi} =$$
$$= \alpha_*\pi\Big[i\omega\big(\zeta_0-\frac{3}{4}\big)-1\Big]$$

The amplitude will therefore be

$$\gamma_0 = \frac{1}{D(\omega)}\alpha_*\pi\Big[i\omega\big(\zeta_0-\frac{3}{4}\big)-1\Big] \tag{6.5}$$

As one can see, if $\zeta_0 = 3/4$, i.e. the centre of stiffness is positioned at $\hat{x} = 3c/4$, the numerator in the expression for γ_0 is independent of the frequency.

6.2 Vertical oscillation of rigid aerofoil

In this case the shape of the aerofoil will not change, only its displacement in the vertical direction. If the amplitude of the aerofoil oscillation is denoted h then

$$\widetilde{Y}_+(x) + \widetilde{Y}_-(x) = 2h$$
$$\frac{d}{dx}(\widetilde{Y}_+(x) + \widetilde{Y}_-(x)) = 0$$

The oscillating part is showed in Figure 6.2. Substituted into (5.6) gives

$$\int_0^1 \sqrt{\frac{\zeta}{1-\zeta}}\Big[i\omega\Big(\widetilde{Y}_+ + \widetilde{Y}_-\Big) + \frac{d}{d\zeta}\Big(\widetilde{Y}_+ + \widetilde{Y}_-\Big)\Big]\,d\zeta = 2i\omega h\int_0^1 \sqrt{\frac{\zeta}{1-\zeta}}\,d\zeta \tag{6.7}$$

which with the same manner as above gives

$$2i\omega h\int_0^1 \sqrt{\frac{\zeta}{1-\zeta}}\,d\zeta = 2i\omega h\Big[u-\frac{1}{2}\sin 2u\Big]_{n\pi}^{\pi/2+n\pi} = i\omega\pi h$$

Hence the amplitude for the velocity jump is given by

$$\gamma_0 = \frac{i\omega\pi h}{D(\omega)} \tag{6.8}$$

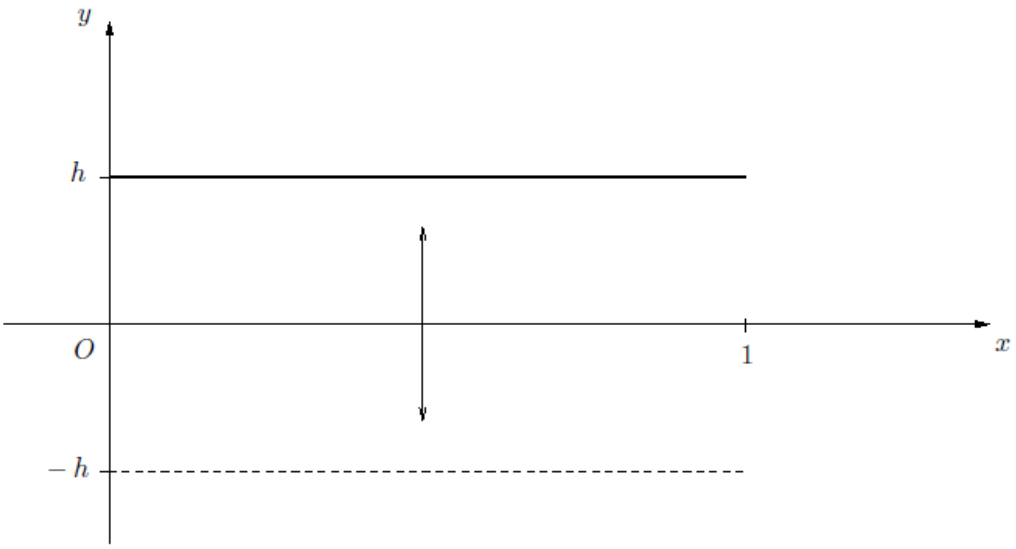

Figure 6.2: Vertical oscillations with amplitude h.

6.3 Aileron flutter

The last case is the case when the aileron is subjected to flutter. In mathematical form this can for a flat plate be written as

$$\widetilde{Y}_{\pm}(x) = \begin{cases} -\alpha_*(x - x_0), & \text{if } x > x_0 \\ 0, & \text{if } x < x_0 \end{cases}$$

since $\widetilde{Y}_{\pm}(x)$ is only the oscillating part and the main body of the aerofoil, which in this case is before x_0, is now rigid and only the aileron oscillates. This is illustrated in Figure 6.3. Substituted into (5.6) gives

$$\int_0^1 \sqrt{\frac{\zeta}{1-\zeta}}\Big[i\omega\Big(\widetilde{Y}_+ + \widetilde{Y}_-\Big) + \frac{d}{d\zeta}\Big(\widetilde{Y}_+ + \widetilde{Y}_-\Big)\Big]\, d\zeta = \int_{\zeta_0}^1 \sqrt{\frac{\zeta}{1-\zeta}}\Big[- 2\alpha_* i\omega\Big(\zeta - \zeta_0) - 2\alpha_*\Big]\, d\zeta$$

Using again $\zeta = \sin^2 u$ gives the amplitude γ_0 to

$$\gamma_0 = \frac{1}{D(\omega)}(-4\alpha_* i\omega\Big[\frac{3u}{8} - \frac{\sin 2u}{4} + \frac{\sin 4u}{32}\Big]_{\sin^{-1}(\pm\sqrt{\zeta_0})}^{\sin^{-1}(\pm 1)} +$$

$$+ 2\alpha_*(i\omega\zeta_0 - 1)\Big[u - \frac{1}{2}\sin 2u\Big]_{\sin^{-1}(\pm\sqrt{\zeta_0})}^{\sin^{-1}(\pm 1)}) \tag{6.9}$$

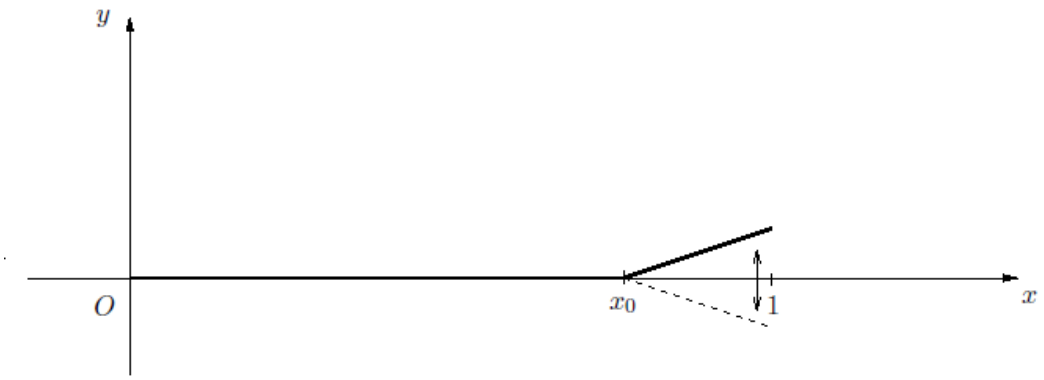

Figure 6.3: Oscillation for aileron.

Chapter 7

Discussion and conclusion

By assuming thin aerofoil, small angle of attack and small perturbation of the discontinuity line modeling the wake, the governing equations for the flow field, the unsteady Euler equations, was linearised together with the boundary conditions in the far distance, the kinematic condition along the aerofoil and the discontinuity line, and the dynamic condition over the discontinuity line. This resulted in that the Euler equations could be rewritten as the Cauchy-Riemann equations, given by (4.4) and (4.5), and therefore showing that there exists an analytic function $f(z)$ with real part being the horizontal displacement $u_1(x, y)$ and imaginary part the vertical displacement with opposite sign $-v_1(x, y)$.

The flow field could therefore be investigated in the complex plane by finding this analytic function $f(z)$, with an appropriate defined branch cut over the aerofoil and the wake, hence removing all discontinuities so that the function $f(z)$ became analytic on the remaining z-plane, as well as with appropriate restrictions on $f(z)$ such that the boundary conditions in the far distance and the kinematic conditions along the aerofoil and wake were satisfied.

It was further shown that the function $f(z)$ could be divided into a sum of two analytic functions, one representing the flow around a symmetric aerofoil, $f_1(z)$, and the other the flow around an anti-symmetric aerofoil, $f_1(z)$, where the contribution of the angle of attack is within the latter one. For investigation of flutter and the wake only the contribution from the anti-symmetric part was needed to be analysed.

A general expression for $f_2(z)$ was achieved by using contour integration, or more precise, Cauchy's integral formula. The contour of integration was chosen in such a way that it included a large enough part of the z-plane to include any interesting points z and the branch cut was excluded. The general expression relating $f_2(z)$ to the function of the velocity jump across the wake was found, given by (4.52).

By comparing this expression to an expression relating $f_2(z)$ to the circulation around the aerofoil achieved by complex potential, a general equation for the velocity jump over the wake was found given by (4.59).

Harmonic oscillations were investigated and the function for the velocity jump was found to be (5.2). A general expression for the amplitude of the harmonic oscillations

is given by (5.6) with (5.7) or Figure 5.1. This expression was evaluated for three types of flutter; twisting oscillations around a point on the aerofoil given by (6.5), vertical oscillations given by (6.8), and aileron flutter given by (6.9).

The assumptions made in this analysis will now be discussed. The choice of neglecting terms of order ε^2, where ε is the thickness, depends on the aerofoil thickness. For normal passenger airplanes this thickness is around 10%, which leads to that only 1% will have been neglected. For airplanes within the army the thickness is even thinner, hence even smaller errors. By linearizing the equations the principle of superposition is still valid, and the results obtained in the previous chapter can simply be superpositioned for a more general case of flutter. The approximation of inviscid flow is good as long as the flow is attached. Regarding the flow being incompressible the results can be changed to compressible flow by using the Prandtl-Glauert transformation, which relates the pressure coefficient in the compressible flow to the pressure coefficient in the incompressible flow by the Mach number. This formula works well for Mach numbers smaller than 0.7 and larger than 1.3, and the pressure in the compressible field can therefore be found for those Mach numbers. Since the velocity field can be achieved as mentioned above, the pressure distribution can be obtained through one of the momentum equations, (3.16a) or (3.16b). Integrating the pressure along the aerofoil surface gives the lift force.

The method presented in this report is both fast and easy, and the errors are on the same level or better than obtained by other methods such as CFD methods, piston theory or wind tunnel experiments.

Bibliography

[1] TH. von Karman and W. R. Sears, *Airfoil Theory for Non-Uniform Motion*, Journal of the Aerodynamical Sciences, Vol. 5, No. 10, pp. 379-390, 1938

[2] M. Munk, *General Theory of Thin Wing Sections*, NACA Report 142, 1922.

[3] T. Theodorsen, *General Theory of Aerodynamical Instability and the Mechanism of Flutter*, NACA Report 496, 1935

[4] H. Glauert, *The Force and Moment on an Oscillating Aerofoil*, Tech. Rep. Aero. Res. Comm. 1242, 1929.

[5] J. Katz and D. Weihs, *Hydrodynamic Propulsion by Large Amplitude Oscillation of an Airfoil With Chordwise Flexibility*, J. Fluid Mech. 88(3). p.485-497, 1978

[6] J. Katz and D. Weihs, *The Effect of Chordwise Flexibility on the Lift of a Rapidly Accelerated Airfoil*, Aeronautical Quarterly. 30. p.360-370, 1979

[7] B.G. van der Wall and W. Geissler, *Experimental and Numerical Investigations on Steady andUnsteady Behaviour of a Rotor Airfoil with a Piezoelectric Trailing Edge Flap*, 55th American Helicopter Society Forum,Montreal, Canada, 1999

[8] M. E. Goldstein and H. Atassi, *A complete second-order theory for the unsteady flow about an airfoil due to periodic gust*, J. Fluid Mech. Vol. 74, part 4, pp. 741-765, 1976

[9] M. S. Triantafyllou, G. S. Triantafyllou and D. K. P. Yue, *Hydrodynamics of Fishlike Swimming*, Annu. Rev. Fluid Mech. 32:33-53, 2000

[10] L. Råde and B. Westergren, *Mathematics Handbook for Science and Engineering.* Studentlitteratur, Lund, Sweden. Fifth edition, 2004. p. 197-198

[11] Lennart Råde and Bertil Westergren, *Mathematics Handbook for Science and Engineering.* Studentlitteratur, Lund, Sweden Fifth edition, 2004. p. 168